

Luis Benet · Olivier Merlo

# Phase-Space Volume of Regions of Trapped Motion: Multiple Ring Components and Arcs

March 8, 2022

**Abstract** The phase–space volume of regions of regular or trapped motion, for bounded or scattering systems with two degrees of freedom respectively, displays universal properties. In particular, sudden reductions in the phase-space volume or gaps are observed at specific values of the parameter which tunes the dynamics; these locations are approximated by the stability resonances. The latter are defined by a resonant condition on the stability exponents of a central linearly stable periodic orbit. We show that, for more than two degrees of freedom, these resonances can be excited opening up gaps, which effectively separate and reduce the regions of trapped motion in phase space. Using the scattering approach to narrow rings and a billiard system as example, we demonstrate that this mechanism yields rings with two or more components. Arcs are also obtained, specifically when an additional (mean-motion) resonance condition is met. We obtain a complete representation of the phase-space volume occupied by the regions of trapped motion.

**Keywords** Phase space volume of trapped regions · Scattering systems · Narrow rings · Multiple components · Arcs

## 1 Aims, motivation and scope

The aim of this paper is two fold: On the one hand, we address the question of the dependence of the phase-space volume of the regions of trapped motion in terms of a parameter that tunes the dynamics. The class of systems we address are dominated by escaping trajectories, i.e. scattering systems, which may exhibit dynamically trapped motion. Examples include Hénon’s map, open billiard systems, scattering maps, the RTBP, among others, i.e., Hamiltonian scattering systems

---

Luis Benet · Olivier Merlo  
Instituto de Ciencias Físicas, Universidad Nacional Autónoma de México (UNAM)  
Apdo. Postal 48–3, 62251–Cuernavaca, Mor., México  
E-mail: benet@fis.unam.mx, merlo@fis.unam.mx

with two and more degrees of freedom. This question was first formulated and answered for bounded Hamiltonian systems of two degrees of freedom in terms of the regions in phase space that exhibit ordered motion (Contopoulos et al. 2005; Dvorak and Freistetter 2005). For two degrees of freedom Hamiltonian systems, the volume in phase-space of the regions of trapped or ordered motion displays universal behavior in terms of a parameter that controls the dynamics (Contopoulos et al. 2005; Dvorak and Freistetter 2005), revealing abrupt changes at specific locations which can be well approximated (Benet and Merlo 2008) and exhibiting self-similar behavior (Simó and Vieira in preparation). Universality means that the same behavior and predictions are obtained for a wide class of systems. Yet, for systems with more than two degrees of freedom there are no results of this type, which therefore calls for attention. The evident difficulty lies in the higher dimensionality of phase space, which prevents the use of standard techniques to distinguish whether an initial condition belongs to a phase space region of ordered or trapped motion or not. We therefore shall study the dependence upon a parameter that tunes the dynamics of the phase space volume of the regions of trapped motion in a specific scattering system with two or two-and-half degrees of freedom.

The second aspect that we address here are the implications of the previous study in the formation of dynamical patterns obtained by projecting the phase-space locations of many non-interacting particles at a given time into the configuration space (real space); we refer to these patterns as rings. More specifically, we consider the appearance of fine structure and its azimuthal dependence in the context of the narrow planetary rings, which are formed by the ensemble of non-escaping particles. Our study is based on the scattering approach (Merlo and Benet 2007), and we use as illustrative example an unrealistic system, namely, a planar circular hard disk whose center moves along a Keplerian closed trajectory. Despite of the non-realistic interactions considered in this example, we do obtain rings which display more than one component and arcs, features which are in qualitative agreement with observations of real narrow planetary rings (for an account of the observations see the recent book by Esposito 2006). The important aspect is not how realistic is the example used, but the fact that the occurrence of structure in these rings, such as multiple components and arcs, is understood and explained in terms of the underlying phase space. The additional costs of integrating more complicated equations of motion may not provide any additional conceptual understanding; this was actually the main motivation for the introduction of billiard systems by Birkhoff (1927).

The reader may ask what is the relevant contribution of our work for the understanding of real planetary rings, bearing in mind that we use a non-realistic system with non-interacting ring particles as example to illustrate our ideas. Indeed, planetary rings are flat self-gravitating systems consisting of many colliding particles (Esposito 2006, cf. chapter 4), which revolve around oblate planets and are perturbed by nearby satellites. The connection of the billiard system with the restricted three-body problem was formally established by Benet (2001) and explicitly illustrated in Merlo and Benet (2007). Briefly, one first includes the central planet at the origin and its gravitational attraction, and then considers the limit of vanishing radius of the disk. It can be shown that this situation is identical to the restricted three-body problem with mass parameter  $\mu = 0$  (Hénon 1968);

in particular, we note that both problems share the simple consecutive-collisions periodic orbits. Hitzl and Hénon (1977) proved that the second species periodic orbits of the restricted three-body problem when  $\mu \rightarrow 0$  are precisely the critical points of the consecutive-collision periodic orbits for  $\mu = 0$ , which correspond to the vanishingly small disk with a central  $1/r$  attractive potential. This shows that our results using the rotating billiard system are indeed connected with more realistic models such as the restricted three-body problem, and that the underlying phase-space structure of these problems is similar. While this point is certainly important, more relevant is the fact that this shows the robustness of the scattering approach. Robustness warranties that we can extend the model beyond the restricted three-body problem, and include the oblateness of the planet as well as other perturbations, e.g., the gravitational influence of other satellites. We refer the reader to Merlo and Benet (2007), where these and other physically relevant aspects of the scattering approach, in particular the predictions in connection to some structural properties of narrow rings, are discussed in detail.

The paper is organized as follows: In the next section we briefly describe the toy-model (or example) we use throughout the paper, a scattering billiard system that moves on a Kepler circular or elliptic orbit. In section 3 we obtain the rings and their structural properties in terms of the eccentricity of the orbit of the center of the disk. In particular, we obtain rings with two or more components which in addition may reveal arcs. In section 4 we relate the fine structure observed in the rings with the specific behavior of the phase space volume of the regions of trapped motion in terms of a parameter that controls the dynamics. Finally, in section 5 we summarize and provide our conclusions.

## 2 The scattering billiard on a Kepler orbit

In this section we briefly describe our toy model, a disk on a Kepler orbit, which is a scattering billiard system (Meyer et al. 1995). This is a simple yet compelling toy model for chaotic scattering (Dullin 1998), which includes the case of more than two degrees of freedom (Benet et al. 2005). In addition, it is the simplest example that illustrates the occurrence of narrow rings within the scattering approach and allows some analytical treatment (Benet and Merlo 2004; Merlo and Benet 2007).

The system consists of a point particle (ring particle) moving freely on the  $X$ - $Y$  plane which may collide with an impenetrable circular hard-disk of radius  $d$ , whose center moves on a Kepler ellipse. Bounces with the disk are treated as usual in the local (moving) reference frame at the point of collision (Meyer et al. 1995); particles that do not bounce with the disk escape inevitably to infinity along scattering trajectories. In the context of rings we are interested in the initial conditions of particles that stay trapped in the system for very long if not infinitely long times. Therefore, bounces with the disk are the only way in which the potential may confine the motion of the ring particles. Note that bounces are necessary, but not sufficient, to avoid escaping to infinity. Hence, we shall focus on the phase space conditions that ensure trapping for a set of initial conditions of positive measure.

Figure 1 illustrates the geometry of the scattering billiard on a Kepler orbit. The center of the disk moves on a circular or elliptic Kepler orbit of semi-major axis  $R = 1$  ( $R > d$ ), the origin being located at one of the foci of the ellipse.

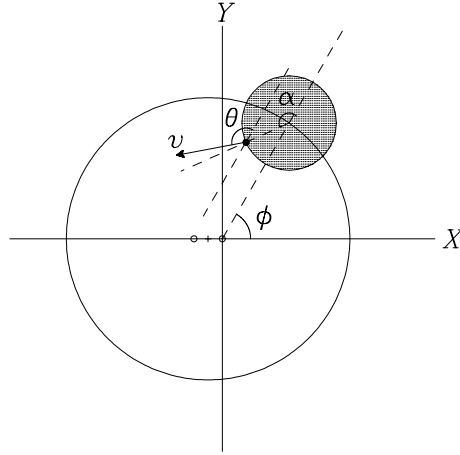


**Fig. 1** The geometry of the scattering billiard on a Kepler orbit:  $\phi$  is the angular position of the center of the disk,  $\alpha$  denotes the position of the collision point on the disk,  $v$  is the magnitude of the outgoing velocity and  $\theta$  defines its direction. The center of the disk moves on a Kepler ellipse, whose foci are shown on the  $X$ -axis as open circles ( $\circ$ ), and its center by a cross ( $+$ ). The shaded circular region is the disk.

We denote by  $\mathbf{X}_d(\phi)$  the position in an inertial frame of the center of the disk in terms of  $\phi$ , the true anomaly (measured from pericenter),  $R_d(\phi)$  denotes the radial component and  $\varepsilon$  is the eccentricity of the orbit. The Hamiltonian of this system in an inertial frame is given by

$$H = \frac{\mathbf{P}^2}{2} + V_d(|\mathbf{X} - \mathbf{X}_d(\phi(t))|). \quad (1)$$

Here,  $\mathbf{X}$  and  $\mathbf{P}$  are the coordinates and the canonically conjugated momenta of the ring particle, respectively, and  $V_d(|\mathbf{X} - \mathbf{X}_d(\phi(t))|)$  is the interaction potential with the disk. The latter is zero if  $|\mathbf{X} - \mathbf{X}_d(\phi(t))| > d$  and infinite otherwise.

For non-zero  $\varepsilon$ , due to the explicit time dependence, the Hamiltonian system has two-and-half degrees of freedom and no constant of motion; for  $\varepsilon = 0$  there is a constant of motion, the Jacobi integral, and the system has only two degrees of freedom. The Jacobi integral is the Hamiltonian expressed in a rotating frame. In general, we may parameterize the phase space of the system by the usual coordinates and momenta for the particle and  $\phi(t)$  for the position of the disk. Yet, since we are interested in the case where the particle is dynamically trapped through collisions with the disk, a simpler parameterization is given as follows. Let  $\alpha$  denote the angular position of the collision point on the disk,  $v$  the magnitude of the outgoing velocity after the collision, and  $\theta$  be the angle defining the outgoing direction of the velocity with respect to the vector  $\mathbf{X}_d(\phi(t))$ . We denote by  $t_i$  the time when the  $i$ -th collision takes place; whenever we shall need to refer to a specific initial condition, we shall use the notation  $t_i^{(k)}$ . Notice that the precise outcome of a collision with the disk depends upon the position on the disk where it occurs, the relative velocities, and for non-vanishing  $\varepsilon$ , on the position on the ellipse where the disk is located at the collision time,  $\phi(t)$ . For circular motion of the disk, collisions taking place on the front of the disk increase the (outgoing)

kinetic energy of the particle, while collisions on the back reduce it. This allows to construct explicitly the simple periodic orbits.

### 3 Narrow rings and fine structure

We are interested in the structural properties of a ring, whenever it occurs. Its occurrence can be understood in simple and general terms within the scattering approach to narrow rings (Merlo and Benet 2007). Basically, we consider the scattering dynamics of an ensemble of non-interacting ring particles that move under the influence of an intrinsic rotation. For the planetary case, the intrinsic rotation corresponds to the time-dependent forces (assumed periodic or quasi-periodic) that originate from the motion of the planetary moons that orbit around the central planet; a solution of the  $N$ -body problem for the planet and moons defines a restricted  $(N + 1)$ -body problem to describe the motion of the ring-particle. The intrinsic rotation creates generically regions in the extended phase space of dynamically trapped motion close to the linearly stable periodic orbits, in what otherwise is dominated by escaping trajectories (Benet and Seligman 2000; Benet 2001). These regions are in general quite small and localized, appearing only in certain bounded regions of the extended phase space. We set the initial conditions of the ensemble of non-interacting particles, the ring particles, in a domain that contains these regions of trapped motion, and let the system evolve for a time which is long enough. Particles that do not belong to these regions escape in short time scales. For the particles that remain trapped, we project their phase-space locations onto the  $X - Y$  plane. The pattern formed is a ring. The ring is typically narrow, sharp-edged and non-circular. These properties follow from the phase-space regions of trapped motion which are rather localized in phase space, the scattering dynamics, and the shape of the organizing centers (periodic orbits) of the regions of bounded motion, respectively (see Merlo and Benet 2007).

The billiard on a Kepler orbit is a good example for illustrating the scattering approach: It allows to certain analytical treatment and the integration of the equations of motion for the billiard system is essentially exact. For the disk on a circular orbit,  $\varepsilon = 0$ , the organizing centers of the dynamics can be explicitly calculated and correspond to the radial consecutive-collision periodic orbits, i.e., those where the kinetic energy stays constant after the collision (Meyer et al. 1995). These radial consecutive-collision orbits can be described in terms of the Jacobi integral  $J$  and the angle  $\theta$  defined above as (Merlo and Benet 2007)

$$J = 2\omega_d^2(R - d)^2(1 + \Delta\phi \tan \theta) \cos^2 \theta (\Delta\phi)^{-2}. \quad (2)$$

Here,  $\Delta\phi = (2n - 1)\pi + 2\theta$  is the angular displacement of the disk between consecutive radial collisions and  $n = 0, 1, 2, \dots$  is the number of full rotations completed by the disk before the next collision. The period of the motion of the disk is  $T_d = 2\pi (\omega_d = 1)$ . We note that the form of Eq. (2) implies that the radial collision periodic orbits appear, in terms of  $J$ , through saddle-center bifurcations, i.e., in pairs, with one linearly stable and the other linearly unstable close enough to the bifurcation point (Benet and Seligman 2000); the bifurcation point is defined by the condition  $dJ/d\theta = 0$ .

For systems with two degrees of freedom, the dynamics can be analyzed using standard methods, e.g., with a Poincaré section. In particular, for  $\varepsilon = 0$  we consider the symplectic map of the surface of section onto itself,  $(\alpha_{k+1}, p_{k+1}) = \mathcal{P}_J(\alpha_k, p_k)$ , defined when the particle collides with the disk, where  $p_k = -d - R \cos \alpha_k - v_k \sin(\alpha_k - \theta_k)$  is kin to the angular momentum (Merlo and Benet 2007). The map is constructed by solving numerically the transcendental equation (using Newton's method to high accuracy) which determines the time for the next collision (see Benet et al. 2005 for details); whenever there is a solution, the resulting outgoing variables are computed. Note that this map is smooth and locally invertible. Linear stability of the radial collision periodic orbits is explicitly given by the trace of the linearized dynamics  $D\mathcal{P}_J$ , which can be obtained analytically (Benet and Merlo 2004; Merlo 2004),

$$\text{Tr}D\mathcal{P}_J = 2 + [(\Delta\phi)^2(1 - \tan^2\theta) - 4(1 + \Delta\phi \tan\theta)]R/d. \quad (3)$$

Then, the radial collision periodic orbits are *linearly* stable iff  $|\text{Tr}D\mathcal{P}_J| \leq 2$ .

For the case of two degrees of freedom,  $\varepsilon = 0$ , close enough to the linearly stable radial collision periodic orbits KAM theorem (Arnold 1988; Nekhoroshev 1977) implies that there exist invariant tori where the motion is quasi-periodic and the set has a positive measure. Note that KAM theorem applies since the map is a Hamiltonian diffeomorphism for almost all  $J$  and the Diophantine condition is fulfilled; actually the theorem can be applied for all values of  $J$  where the linearly stable radial periodic orbits has complex eigenvalues  $\lambda$  in the unit circle such that  $\lambda^2 \neq 1$ ,  $\lambda^3 \neq 1$ ,  $\lambda^4 \neq 1$  and the first coefficient of the resonant normal form is non-zero (Duarte 1994). Clearly, the KAM-tori are trapped orbits, which also holds for the regions of chaotic motion that are bounded by those KAM tori. More important, the invariant manifolds of the external unstable fixed point define a bounded region, which contains the stable fixed point. This region contains a domain where the motion is strictly bounded or dynamically trapped, i.e., where the corresponding trajectories cannot escape to infinity. We consider the whole interval of  $J$  where such regions exist; for concreteness we focus in the  $n = 0$  radial collision periodic orbit, cf. Eq. (2), which corresponds to the largest region of trapped motion in phase space. We proceed as described above to obtain the ring, which is illustrated in figure 2. In the figure we included analytical estimates for the borders based on the projection of the curves  $\text{Tr}D\mathcal{P}_J = \pm 2$ , which are the limits for having linearly stable radial-collision periodic orbits. The resulting ring is narrow, eccentric, displays sharp-edges and the estimates based on linear stability are excellent.

We turn now to the case of non-zero eccentricity. The explicit time dependence of the elliptic Kepler motion cannot be removed, not even by canonically transforming to a pulsating–rotating frame (which defines the generalized Jacobi integral). Therefore, the Hamiltonian system has two-and-half degrees of freedom and no constants of motion. In this case the invariant tori do not separate regions in phase space and new phenomena like Arnold diffusion may appear (Arnold 1964). In spite of this, regions of trapped motion do exist at least in the sense of effective or practical stability, i.e., for very long but maybe not infinite times (see Jorba and Villanueva 1997a,b). We checked this by considering a large number of consecutive bounces in the numerical experiments (ring particles must display at

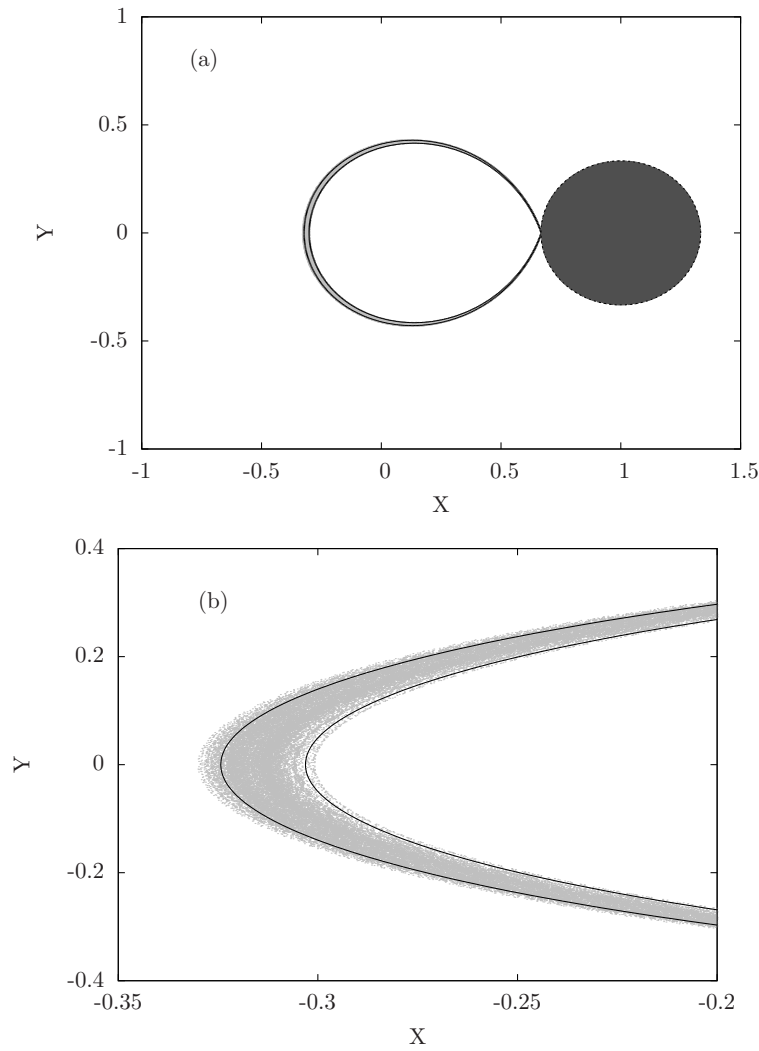


**Fig. 2** (a) Stable ring of non-interacting particles of the billiard on a circular orbit for the  $n = 0$  stable periodic orbit at a given time. The dark shaded circular region is the disk. (b) Detail of a region of the ring. The black lines are the analytical estimates given by  $\text{Tr} D\mathcal{P}_J = \pm 2$ .

least 100000 collisions with the disk to be considered trapped), and by confirming the appearance of a non-statistical peak in the decay-rate statistics (see Merlo 2004; Benet et al. 2005 for details). Therefore, the theory can indeed be extended to systems with more degrees of freedom in terms of (a) the stable tori as the organizing centers of the dynamics and, (b) the regions of bounded motion that are found close to them which are defined now at least on an effective stability sense (Merlo and Benet 2007). Rings are then obtained by the construction described above.

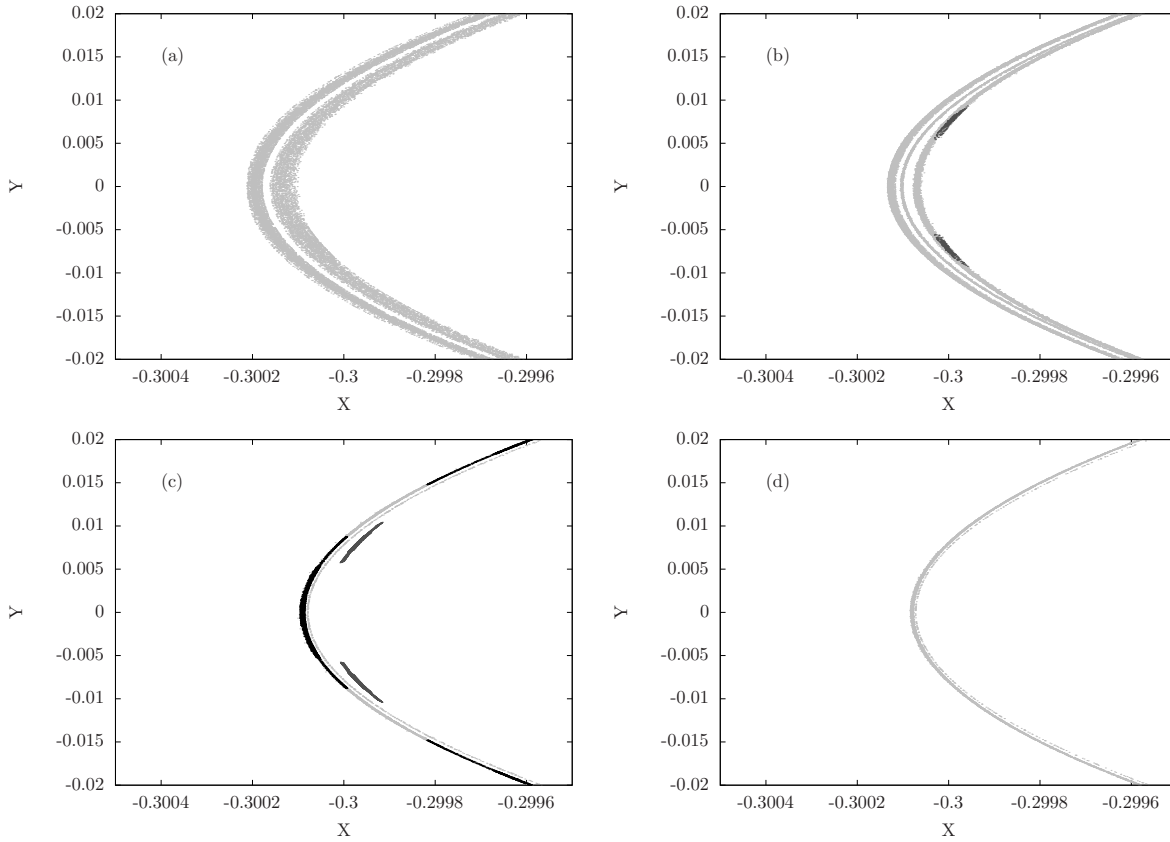


**Fig. 3** Details of a region of the  $n = 0$  ring for (a)  $\varepsilon = 0.00165$ , (b)  $\varepsilon = 0.00167$ , (c)  $\varepsilon = 0.00168$  and (d)  $\varepsilon = 0.001683$ . In (b) and (c) we have distinguished bunches of particles which move as such, i.e., without spreading throughout the corresponding strand. These bunches of particles mark the occurrence of arcs or clumps in the ring.

For extremely small values of  $\varepsilon$  the ring is similar to its counterpart for the circular case, except that it is narrower, i.e., the regions of trapped motion become smaller in phase space by increasing the eccentricity. But breaking the circular symmetry has consequences in the structural properties of the ring beyond its narrowness. In Figs. 3 we plot a detail of the  $n = 0$  ring for slightly different values of  $\varepsilon$ : The rings display multiple components (strands) and incomplete rings (arcs). Indeed, Fig. 3(a) shows a ring with two strands, the ring in Fig. 3(b) has three, and the rings of Figs. 3(c) and (d) have again two components. The different strands actually are entangled among each other (see Merlo and Benet 2007) in what reminds us the braids observed in the F ring of Saturn (Esposito 2006). In addition, in Figs. 3(b) and (c) we observe the appearance of arcs within the ring, which we have distinguished in the figures as the dark grey clumps. In Fig. 3(b) the arcs appear immersed in the innermost strand, while in Fig. 3(c) that strand has disappeared allowing us to unambiguously identify the corresponding arcs. These structures are evocative of Adam's arcs observed in Neptune and of the sets



of clumps observed in some ringlets in Saturn (Esposito 2006). In Fig. 3(c) we have also succeed to identify another set of arcs which appear embedded in the outermost strand; in Fig. 3(d) there are no arcs embedded in the rings.

The small difference in the eccentricity in the last three cases indicates that the structural properties of the ring depend very sensitively of the precise value of  $\varepsilon$  in this model. Furthermore, breaking the circular symmetry induces a strong azimuthal dependence in the regions of trapped motion in phase space, as manifested by the arcs. These structural properties of the ring are related to specific phase-space aspects of systems with more than two degrees of freedom.

## 4 Phase space volume of the regions of trapped motion

### 4.1 Two degrees of freedom and stability resonances

The Hamiltonian system which gives rise to rings revealing multiple components and arcs (Figs. 3) corresponds to an explicitly time-dependent Hamiltonian, a system with two-and-half degrees of freedom. Our aim is to characterize the regions of trapped motion and the phase space properties where the ring particles actually move, and as we have seen, yield rings with azimuthal structure.

To this end, we consider a relative measure of the phase-space volume occupied by the regions of trapped motion. For scattering systems in particular, the volume of the regions of trapped motion depends on the degree of development of the invariant horseshoe (Rückerl and Jung 1994). Therefore, the volume of the regions of trapped motion is a function of any parameter which tunes the development of the horseshoe or that manifests it. For the rotating disk in a circular orbit a good choice is obviously the Jacobi integral. Yet,  $J$  is not conserved when  $\varepsilon$  differs from zero, thus becoming useless. A convenient quantity in this case is the average time between consecutive collisions with the disk,  $\langle \Delta t \rangle$ . Notice that  $\langle \Delta t \rangle$  is precisely the average return time to the surface of section. Defining the control parameter in this way is convenient since it may be generalized to any Hamiltonian system independently of the number of degrees of freedom.

We use  $t_i^{(k)}$  to denote the time of the  $i$ -th collision with the disk for a particle labeled by  $k$  that remains trapped, and  $\langle \Delta t^{(k)} \rangle = (t_N^{(k)} - t_0^{(k)})/N$  its average collision time after  $N$  bounces; we further average over many initial conditions of the ring particles ( $k \gg 1$ ) to obtain  $\langle \Delta t \rangle$ . Numerically, we consider that the initial conditions of a ring particle belong to a region of trapped motion if the particle displays more than 10000 collisions with the disk; we used the next  $N \geq 17500$  collisions for the statistics. Figure 4 shows the frequency histogram of  $\langle \Delta t \rangle$ ; the corresponding region of trapped motion yields the ring of Fig. 2.

The structure shown in Fig. 4 is universal for Hamiltonian systems with two degrees of freedom (Contopoulos et al. 2005; Dvorak and Freistetter 2005). Universality implies that it holds for a wide class of systems. The characteristic feature of Fig. 4 is the occurrence of specific values of the parameter where an abrupt reduction of the phase-space volume of the regions of trapped motion is observed, henceforth referred as gaps. Gaps are observed at every scale and display self-similar structure (Simó 2006, 2007; Simó and Vieiro in preparation). The abrupt changes in phase space can be understood, for two degrees of freedom, from the

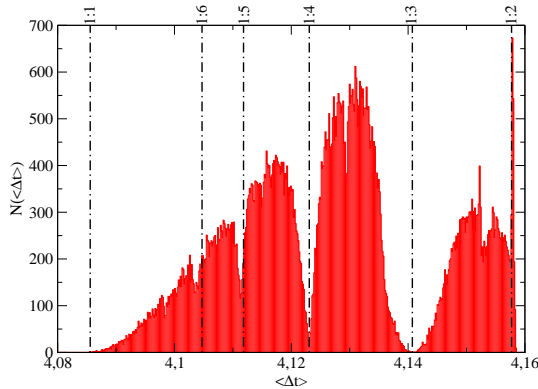


**Fig. 4** Histogram of the average time between consecutive collisions  $\langle \Delta t \rangle$  for an ensemble of particles of the ring of Fig. 2, for the rotating billiard on a circular orbit. The histogram represents a relative measure of the phase-space volume of the regions of trapped motion. The main gaps observed are related to the stability resonances indicated by dash-dotted lines. The structure displayed is universal for Hamiltonian systems of two degrees of freedom.

existence of an outer invariant curve which serves as barrier, thus confining the motion of a region in phase space. Small changes of the parameter destroy such invariant curves, which thus allow the particles within certain region in phase space to escape. This explains the sudden variation in the phase-space volume of the regions of trapped motion observed. See Simó (2007) for a careful analysis of these aspects in Hénon’s map.

Figure 4 provides a *global* description of the region of trapped motion in phase space for  $n = 0$ , i.e., it includes a continuous interval of  $J$  and regions of phase space that do not need to be close to each other. An accurate estimation for the location of the gaps is provided by the stability resonances. The stability resonances are defined by the occurrence of a resonant condition (a rational ratio of  $2\pi$ ) of the linear stability exponents of the central linearly stable periodic orbit. Therefore, they are related to the *local* stability properties of the central stable periodic orbit (Benet and Merlo 2008). Note that the stability resonances must not correspond to mean-motion resonances, which are defined as a rational ratio between the period of the central stable periodic orbit and the period of the disk.

For the rotating disk on a circular orbit the stability of the radial collision periodic orbits is obtained using Eq. (3). We write the eigenvalues of the linearized dynamics  $D\mathcal{P}_J$  for the (linearly) stable radial collision periodic orbit as  $\lambda_{\pm} = \exp[\pm i\eta_{\pm}]$ . The stability resonances are thus defined by the condition  $\eta/(2\pi) = p/q$  with  $p$  and  $q$  incommensurate integers. From the definition of the (imaginary) eigenvalues  $\lambda$  it follows  $\cos \eta = \text{Tr} D\mathcal{P}_J/2$ , which can be written in terms of the collision time  $t_{\text{col}} = \Delta\phi/\omega_d$  using Eq. (3). Notice that the eigenvalues  $\lambda_{\pm}$  are related to each other by complex conjugation; by consequence, the  $p : q$  resonance is related to the  $q - p : q$  resonance. In Fig. 4 we have indicated the location of some lower-order stability resonances as dash-dotted vertical lines. The

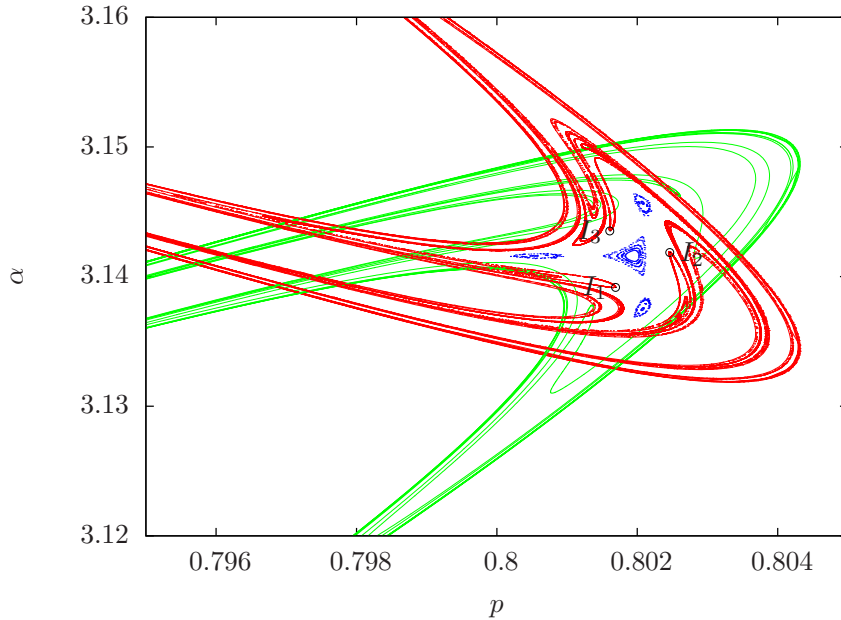


**Fig. 5** Surface of section for the billiard system on a circular orbit with  $J/(R-d)^2 = 0.293011$ . The labels indicate subsequent tips of the unstable manifold. Note that these tips mimic the periodicity of the period-three unstable periodic orbit associated with the secondary islands displayed.

correspondence with the gaps is excellent, though not perfect, as illustrated by the 1:5 or 1:6 stability resonances. The reason that there is no perfect correspondence of the gaps and the stability resonances is related to the fact that the latter are defined using a local estimate of the stability of the central (linearly) stable periodic orbit. Changing slightly the control parameter changes accordingly the stability properties of this periodic orbit. In turn, the phase-space volume of the regions of bounded motion is determined, as mentioned earlier, by the outer invariant curve which bounds the region. The existence of this invariant curve depends subtly on the specific value of the control parameter and thus a change in the control parameter has a global effect.

It is interesting to note that using a local estimate we obtain a good approximation for the location of the gaps, at least in the case of low order stability resonances, recalling that these gaps uncover global aspects of the phase space. To understand how local estimates can provide knowledge on global aspects of the dynamics, we observe that the stability resonances are related to rational winding numbers close to the (linearly) stable periodic orbit. In turn, the phase-space volume of the regions of trapped motion are ultimately related to the invariant manifolds of the unstable periodic orbit and their homoclinic connections, i.e., the underlying horseshoe structure. The connection among these aspects, for low developed horseshoes, can be established by the relation between the *formal development parameter* which characterizes the horseshoe development (Jung et al. 1999) and the characteristic period of an outermost stable periodic orbits (Jung et al.

2004). In particular, notice that certain segments of the manifolds of the unstable periodic orbit (at a locally turning point of the manifolds or tips) are quite close to the unstable periodic orbits that are the companions of the outermost secondary islands, thus mimicking the periodicity of such islands. For low order stability resonances where the change in the phase space volume occupied by trapped trajectories is very drastic, these manifolds do enter deep enough the horseshoe structure and become very close to the linearly stable periodic orbit. This describes the connection of a global property of the phase space with local estimates, which is illustrated in Fig. 5 close to the minimum of the 1 : 3 stability resonance. Conversely, if the invariant manifolds lie somewhat outside the surroundings of the stable periodic orbit, the estimate becomes less accurate.

From Fig. 5, we obtain that the formal development parameter is  $\beta = 1/4$ . This value of  $\beta$  is related with the period  $T_\beta = 3/2 - \log_2 \beta = 3.5$  given in units of the average return time to the surface of section (see Jung et al. 2004). As noted in Jung et al. 2004,  $T_\beta$  is an average period with an associated error of  $\pm 0.5$ . As we approach further the minimum of the histogram associated with the 1 : 3 stability island,  $\beta$  increases slowly and  $T_\beta$  approaches the expected value of three, which corresponds to  $\beta = 2^{-3/2}$ . Notice that this value is well beyond the value  $\beta = 3/8$ , which is known to have problems with respect to a consistent definition of the development parameter R uckerl and Jung (1994). A more detailed study of this will be presented elsewhere.

As mentioned above, for systems with two degrees of freedom the structure of the phase-space volume occupied by regions of trapped motion (Fig. 4) is universal and displays self-similar structure. Universality is a consequence of generic aspects of the dynamics and of the normal form (Arnold 1989; Gelfreich 2002). In particular, the passage through the 1:3 stability resonance leads universally to local instabilities which decrease violently the phase-space volume occupied by trapped orbits, yielding a very small but not necessarily zero phase-space volume of the region of trapped motion. Resonances of order higher than 4 do not induce such strong local instabilities; for the 1:4 stability resonance the behavior depends upon which contribution, resonant or non-resonant, dominates the normal form (see Arnold 1989). These results follow from the structure of the resonant normal form, i.e., the relevant nonlinear contributions to the stability analysis of a central linearly stable periodic orbit, and the scenario of development of the horseshoe.

#### 4.2 Beyond two degrees of freedom: Strands and Arcs

The gaps defined by the stability resonances at first sight seem not to be important for the structure of the ring. For the disk on a circular orbit, they do manifest in the ring's density profile. For non-zero  $\varepsilon$  the relative measure of the phase-space volume occupied by regions of trapped motion displays new features, and this change is manifested in the structure of the corresponding ring. Figure 6(a) illustrates the structure of the phase-space volume of the regions of trapped motion for  $\varepsilon = 0.0001$ . Note that the gaps corresponding to the 1:3 and 1:6 stability resonance are wider and divide the histogram in three regions. We assign different plotting characters to initial conditions belonging to these regions; Fig. 6(b) illustrates the

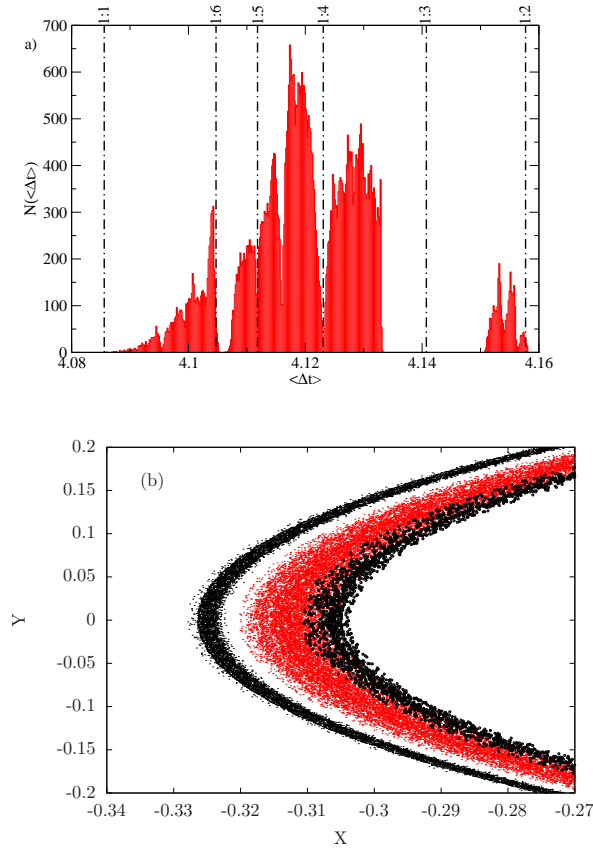


**Fig. 6** (a) Same as Fig. 4 for the billiard on an elliptic Kepler orbit for  $\varepsilon = 0.0001$ . The resonances indicated correspond to  $\varepsilon = 0$ . (b) Detail of the corresponding ring. The gap of the 1:3 stability resonance is wider, which causes a division of the ring thus forming a two-component ring. The innermost component of the ring corresponds to the region on the left of the 1:6 stability resonance, and the middle one to the region between the 1:6 and 1:3 resonances.

ring obtained. The ring displays two components, separated by a ring division, which are entangled and form a braided ring.

We observe that each ring component is related to a different region of the histogram. This is a consequence of the large gap opened by the 1:3 stability resonance, which effectively separates the phase space regions of trapped motion in two disjoint regions (Benet and Merlo 2008). Yet, while the 1:6 stability resonance widens up its corresponding gap, it does not separate *enough* the phase-space regions around it. The rings formed separately (by projection into the  $X - Y$ ) of these regions manifest a clear segregation of ring particles, except for a thin strip. In Figs. 7 we present the relative measures of the phase space volume occupied by the regions of trapped motion for the values of  $\varepsilon$  corresponding to the rings shown in Fig. 3. As in the case  $\varepsilon = 0.0001$ , the stability resonances induce instabilities

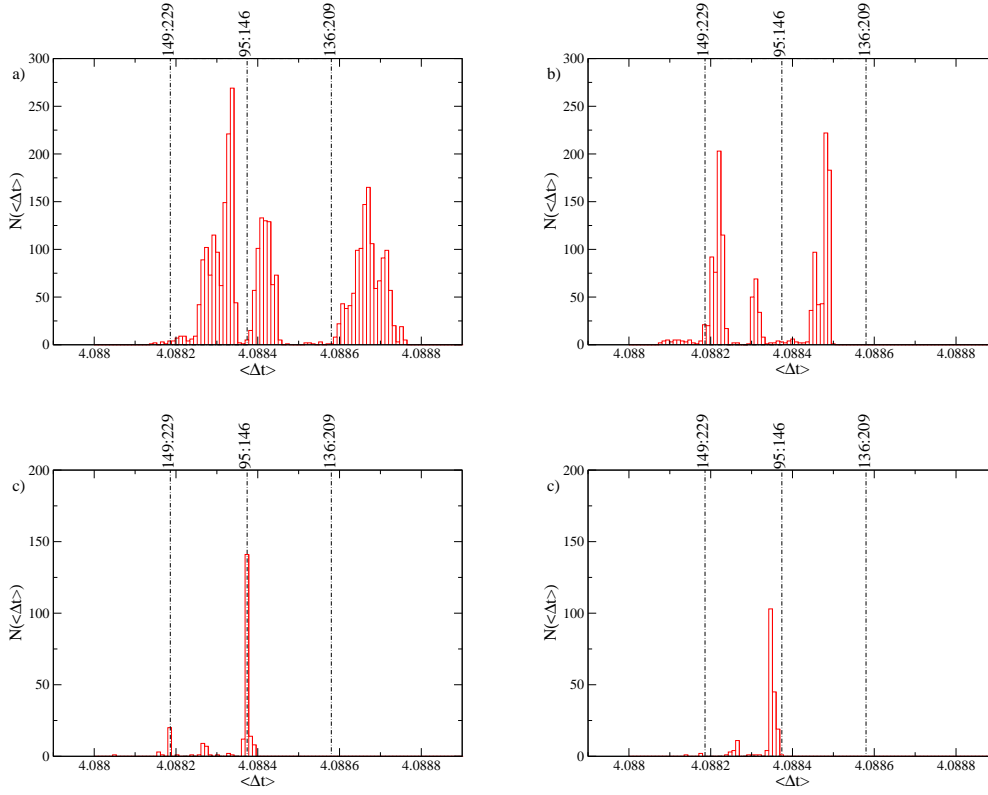


**Fig. 7** Same as Fig. 4 for (a)  $\varepsilon = 0.00165$ , (b)  $\varepsilon = 0.00167$ , (c)  $\varepsilon = 0.00168$  and (d)  $\varepsilon = 0.001683$ , which correspond to the rings given in Fig. 3. Some mean-motion resonances occurring in the interval of  $\langle \Delta t \rangle$  are indicated by dashed-dotted lines. Some of these are related to the appearance of arcs.

which widen up the gaps of the case  $\varepsilon = 0$ . This destroys locally the trapping mechanism in certain regions in phase space and yields one or more divisions of the ring. Therefore, multiple ring components are obtained by exciting the stability resonances through non-zero eccentricity. Note that these structural properties follow from the higher dimensionality of phase space and nonlinear effects, i.e.  $\varepsilon \neq 0$ .

The histograms of  $\langle \Delta t \rangle$  representing a relative measure of the phase-space volume of the regions of trapped motion and the stability resonances clarify the origin of the multiple components of the ring but do not explain the occurrence of arcs. To understand their origin, we first observe that there are *exactly* 149 arcs along the whole ring for  $\varepsilon = 0.000167$ , (Fig. 3(b)). Secondly, the exact angular configuration of the arcs (numbered in an arbitrary way with respect to one ring particle) is repeated after 229 bounces with the disk. This observations leads us to suspect that the appearance of arcs is related to the occurrence of mean-motion resonances. To check this, we have plotted in Figs. 7 the position of the 149:229 mean-motion resonance, i.e.,  $\langle \Delta t \rangle / (2\pi) = 149/229$ . We note that for  $\varepsilon = 0.000168$  the his-

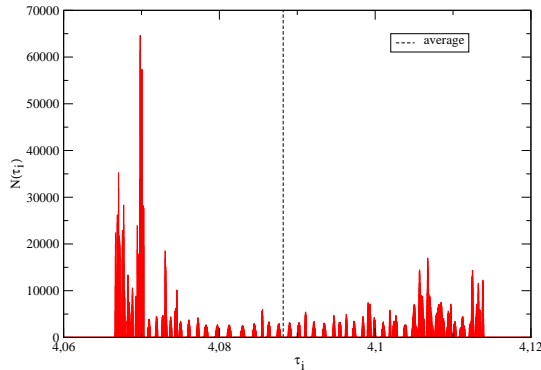


**Fig. 8** Histogram of the time between two consecutive collisions  $\tau_i$  with the disc for one initial condition which belongs to an arc. The average time is indicated by a dashed line.

togram of the phase space volume of the region of trapped motion indicates that there is a region of trapped motion, which is quite narrow, precisely agreeing with the condition for the mean-motion resonance. In this case, arcs are clearly manifested in Fig. 3(c). The same analysis indicates that these arcs are expected for  $\varepsilon = 0.000167$  since this mean-motion resonance is embedded within a region of trapped motion, see Fig. 7(b). We indeed confirmed this expectation as illustrated in Fig. 3(b). The fact that the region of trapped motion is somewhat wide (in the  $\langle \Delta t \rangle$  interval) is the reason for the ring component to be covering the arcs. A similar analysis can be carried out for other resonances. In particular, the 95:146 resonance also occurs inside the  $\langle \Delta t \rangle$  range of interest. We find that this resonance shows up for  $\varepsilon = 0.000168$ , but is embedded within a region of trapped motion, see Fig. 7(c). As shown in Fig. 3(c), in this case the arcs are also embedded inside a ring component.

In Fig. 8 we plot the histogram of elapsed time between consecutive collisions,  $\tau_i = t_i - t_{i-1}$ , for one initial condition that belongs to a specific arc. The figure shows a number of bumps which are clearly separated from each other, and their average value. The histogram demonstrates that the motion of a ring particle within an arc is more constrained than within a ring component, which is consistent with the restriction imposed by the mean-motion resonance condition.

To have a physical picture of the phase space structure we define the Poincaré map from the dynamics on a surface of section which corresponds to collisions with the disc. A periodic orbit in a  $p : q$  mean-motion resonance is a fixed point of  $q$  iterations of the Poincaré map. In the case of circular orbit of the disk, the symmetric case, a whole family of these periodic orbits exist and can be parameterized by the angle  $\phi$  where the particle hits the disc. For small non-vanishing  $\varepsilon$  the  $p : q$  family of periodic orbits persist. Depending on the location in the orbit of the disk  $\phi(t)$  where the bounce takes place the orbits may be stable or unstable (Merlo 2004; Benet et al. 2005), i.e., there is an azimuthal dependence in the stability properties of the periodic orbits. Unstable periodic orbits yield either

a thin layer of chaotic motion within the region of trapped motion, or escaping channels. The stable ones define individual secondary regions of bounded motion, which are separated by the unstable orbits and their associated invariant structures, the projection of each one yielding an individual arc. Figure 8 is a different view of this effect. These secondary regions of bounded motion may be embedded within the main one or may appear as satellite islands of stability. In the former case the arcs overlap with the main strands (cf. Figs. 3(c) and 7(c)); in contrast, in the latter case some arcs may show up as completely separated from strands (cf. Figs. 3(c) and 7(c)). The scenario described above resembles the typical Poincaré-Birkhoff type of structure found in Hamiltonian systems of two degrees of freedom, at least on an effective stability sense for more than two degrees of freedom. We emphasize that arcs manifest an azimuthal dependence in the structure of the ring, which can be understood in these terms.

The above considerations lead us to conclude that two conditions must be satisfied for the occurrence of arcs: First, a mean-motion resonance condition must be met, which in a way allows for the appearance of Poincaré-Birkhoff-like phase-space structures and, secondly, the regions of trapped motion should be thin enough. The last condition is needed to distinguish the arcs from the main ring components. In principle, any high-order mean motion resonance may be observable as a chain of arcs. Yet, numerically, we deal with a finite number of particles distributed in a rather extended region of a higher dimensional phase space. Then, it is a difficult task to distinguish from the structure of the obtained ring if the particles move in individual packets that form the arcs or within a connected ring component.

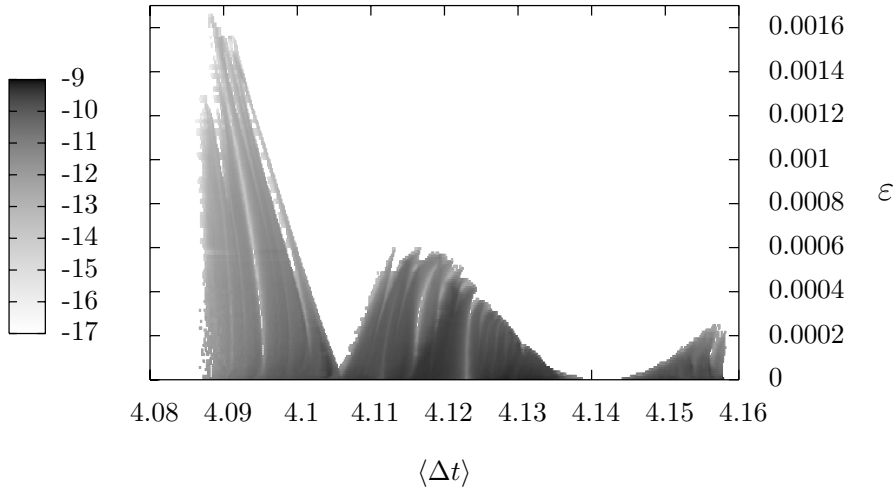
We finish this section showing the combined dependence upon  $\varepsilon$  and  $\langle \Delta t \rangle$  of the phase-space volume of the regions of trapped motion. Figure 9 displays this dependence as a contour plot of the logarithm of the phase-space volume of the regions of trapped motion. For each  $\varepsilon$  computed, we normalized the corresponding histogram to the actual value of the phase-space volume occupied by regions of trapped motion for that case. Typically we have used about 50000 initial conditions to obtain the histogram for a given  $\varepsilon$ , except for higher eccentricities where we have used a smaller number due to the immense time required to obtain a representation of the higher-dimensional phase-space region in question.

Figure 9 manifests the evolution of individual strands when the eccentricity is changed. For a specific strand, the grey tones represent the relative phase-space volume as a function of the eccentricity. The plot also shows which of the stability resonances of the circular case are excited, and actually the whole evolution of these resonances in terms of  $\varepsilon$ . Clearly Fig. 9 provides a global picture in parameter space of the phase-space volume of the regions of trapped motion. Using it allows, among other, to search for  $\varepsilon$  values where arcs manifest.

## 5 Summary and conclusions

In this paper we have studied the phase-space volume of the regions of trapped motion in a specific Hamiltonian system of two and two-and-half degrees of freedom depending on a parameter, an impenetrable hard disk whose center moves on a Kepler orbit with fixed eccentricity (Benet and Merlo 2004; Merlo and Benet 2007). We have also related the phase-space volume of the regions of trapped





**Fig. 9** Contour plot for the representation of the logarithm of the volume of phase space occupied by regions of trapped motion, in terms of the eccentricity  $\varepsilon$  and  $\langle \Delta t \rangle$ . For fixed  $\varepsilon$ , the histogram was normalized to the actual value of the volume of phase space occupied by regions of trapped motion.

motion to the structural properties of the patterns obtained by projecting into the  $X - Y$  plane, at a fixed time, the phase-space locations of an ensemble of particles whose initial conditions belong to these regions of trapped motion. These patterns form ring structures similar to the observed in narrow planetary rings, being non-circular and displaying sharp-edges. These structural properties follow directly from the scattering approach (Merlo and Benet 2007).

For non-zero eccentricity, the rings may display strands and arcs. Multiple ring components are due to the separation of phase-space regions of trapped motion, obtained by widening up the gaps observed in the histograms representing the phase-space volume of the regions of bounded motion. The location of these gaps is approximated by a resonant condition on the stability exponents of the linearized dynamics around a central linearly-stable periodic orbit. This local estimate yields very good results for the low order resonances, while for higher ones the approximation is less accurate; this is due to global effects related to outer invariant curves that define the region of bounded motion, which are not well described by the local estimate. Arcs are observed whenever an additional resonant condition is imposed: a mean-motion resonance. This result represents an independent confirmation that such resonant mechanisms indeed yield corotation sites in phase space (Goldreich et al. 1986). This is in agreement with the current understanding of Adam's arcs in Neptune (Porco 1991; Namouni and Porco 2002), which require to take into account the gravity of the arcs to match recent observations (Sicardy 1999; Dumas et al. 1999). Actually, our results show that different

specific resonances can coexist, and thus yield arcs with different angular widths. We emphasize that both, strands and arcs, are obtained from setting the initial conditions for the ring particles in an interval that contains the regions of trapped motion, and are not imposed artificially. These structural properties are consequences of the high-dimensional and non-linear aspects of the dynamics, in the sense that individual strands and arcs do not occur for Hamiltonian systems with two degrees of freedom. The fact that we obtain them in such a non-realistic system like the hard-disk moving on a Kepler orbit make us confident of the applicability of these ideas in realistic situations.

Our results provide a complete representation of the phase-space volume of the regions of trapped motion for a Hamiltonian system of more than two degrees of freedom. The natural question that arises is whether its structure and properties hold universally for systems with more than two degrees of freedom. In particular, we may ask if the gaps associated with the 1:3 and the 1:6 stability resonances are *always* excited first with respect to variations of the relevant symmetry-breaking parameter, and what intrinsically distinguishes the instability of the 1:6 gap with respect to the 1:5, or put differently, why do other gaps not separate so efficiently. Another interesting question is related to improve the simple estimates given by the stability resonances for the location of the gaps in the histograms of the phase-space volume occupied by trapped orbits, especially for the case of higher-order stability resonances. These questions remain open. We do think that the behavior of the 1:3 stability resonance holds in general: The 1:3 stability resonances are optimally excited by the symmetry-breaking parameter, and we expect to have a sensitive separation of the regions of trapped motion in phase space under small changes of the symmetry-breaking parameter. This is based on the particularly deep gap observed around this resonance for the case where the symmetry holds (two degrees of freedom).

The fact that the rings of the scattering billiard on a Kepler orbit display qualitative similarities to the narrow planetary rings consistently is encouraging: The scattering approach, which is based on the relevant phase-space structures, yields structured rings in qualitative agreement with the observations. The motivation to continue along these lines for systems with more than two degrees of freedom, for example, is to build a theory upon which we can determine or predict the limits of stability that define the regions of trapped motion, and then obtain semi-analytical estimates for the edges of the ring.

**Acknowledgements** We acknowledge financial support provided by the projects IN-111607 (DGAPA-UNAM) and 79988 (CONACyT). We are thankful to Àngel Jorba and Carles Simó for discussions and comments, and Fathi Namouni for critical remarks. O. Merlo is a postdoctoral fellow of the Swiss National Foundation (PBBS2-108932).

## References

- Arnold, V.: 1964, "Instability of dynamical systems with several degrees of freedom", *Sov. Math. Dokl.* **5**, 581–585.
- Arnold, V.I.: 1989, *Mathematical Methods of Classical Mechanics*, (Springer-Verlag, New York), appendix 7.

- Benet, L.: 2001, "Occurrence of planetary rings with shepherds", *Celest. Mech. Dynam. Astron.* **81**, 123-128.
- Benet, L., and Merlo, O.: "Phase-space structure for narrow planetary rings", *Regular and Chaotic Dynamics* **9**, 373-384, arXiv:nlin.CD/0410028.
- Benet, L., and Merlo, O.: 2008, "Multiple Components in Narrow Planetary Rings", *Phys. Rev. Lett.* in press; arXiv:nlin/0702039v2.
- Benet, L., and Seligman, T. H.: 2000, "Generic occurrence of rings in rotating scattering systems", *Phys. Lett. A* **273**, 331-337, arXiv:nlin.CD/0001018.
- Benet, L., Broch, J., Merlo, O., and Seligman, T. H.: 2005, "Symmetry breaking: A heuristic approach to chaotic scattering in many dimensions", *Phys. Rev. E* **71**, 036225.
- Birkhoff, G.D.: 1927, "On the periodic motions of dynamical systems", *Acta Math.* **50**, 359-379.
- Contopoulos, G., Dvorak, R., Harsoula, M., and Freistetter, F.: 2005, "Recurrence of Order in Chaos", *Int. J. Bif. Chaos* **15**, 2865-2882.
- Dvorak, R., and Freistetter, F.: 2005, "Orbit Dynamics, Stability and Chaos in Planetary Systems", in *Chaos and Stability in Planetary Systems*, Lect. Notes Phys. **683** (R. Dvorak, F. Freistetter and J. Kurths, Eds.), pp 3-140 (Springer, Berlin, 2005).
- Duarte, P.: 1994, "Plenty of elliptic islands for the standard family of area-preserving maps", *Ann. Inst. Henri Poincaré* **11**, 359-409.
- Dullin, H.R.: 1998, "Linear Stability in billiards with potential", *Nonlinearity* **11**, 151-173.
- Dumas, C., et al.: 1999, "Stability of Neptune's ring arcs in question", *Nature* **400**, 733-735.
- Esposito, L. W.: 2006, "Planetary rings", (Cambridge University Press, Cambridge).
- Gelfreich, V.: 2002 "Near strongly resonant periodic orbits in a Hamiltonian system", *Proc. Nac. Acad. Sci.* **99**, 13975-13979.
- Goldreich, P., Tremaine, S., Borderies, N.: 1986, "Towards a theory for Neptune's arc rings", *AJ* **92**, 490-494.
- Hénon, M.: 1968, "Sur les Orbites Interplanétaires qui Rencontrent Deux Fois la Terre", *Bull. Astron. (serie 3)* **3**, 337-402.
- Hitzl, D. L., and Hénon, M.: 1977, "Critical generating orbits for second species periodic solutions of the restricted problem", *Celest. Mech.* **15**, 421-452.
- Jorba, A., and Villanueva, J.: 1997a, "On the Normal Behaviour of Partially Elliptic Lower Dimensional Tori of Hamiltonian Systems", *Nonlinearity* **10**, 783-822.
- Jorba, A., and Villanueva, J.: 1997b, "On the persistence of lower dimensional invariant tori under quasi-periodic perturbations", *Journal of Nonlinear Science* **7**, 427-473.
- Jung, C., Lipp, C., Merlo, O., and Seligman, T.H.: 1999, "The inverse scattering problem for chaotic systems", *Ann. Phys.* **275**, 151-189.
- Jung, C., Mejía-Monasterio, C., Merlo, O., and Seligman, T.H.: 2004, "Self-pulsing effect in chaotic scattering", *New J. Phys.* **6**, 48.
- Merlo, O.: 2004, *Through symmetry breaking to higher dimensional chaotic scattering*, PhD Thesis, U. Basel, Switzerland, unpublished. Online version available at [http://pages.unibas.ch/diss/2004/DissB\\_7024.htm](http://pages.unibas.ch/diss/2004/DissB_7024.htm).
- Merlo, O., and Benet, L.: 2007, "Strands and braids in narrow planetary rings: A scattering system approach", *Cel. Mech. Dyn. Astron.* **97**, 49-72, arXiv:astro-ph/0609627.
- Meyer, N., et al.: 1995, "Chaotic scattering off a rotating target", *J. Phys. A: Math. Gen.* **28**, 2529-2544.
- Namouni, F., and Porco, C.: 2002, "The confinement of Neptune's ring arcs by the moon Galatea", *Nature* **417**, 45-47.
- Nekhoroshev, N.N.: 1977, "An exponential estimate of the time of stability of nearly-integrable Hamiltonian systems", *Russ. Math. Surv.* **32**, 5-66.
- Porco, C.C.: 1991, "An explanation for Neptune's ring arcs", *Science* **253**, 995-1001.
- Rückerl, B., and Jung, C.: 1994, "Scaling properties of a scattering system with an incomplete horseshoe", *J. Phys. A: Math. Gen.* **27**, 55-77.
- Sicardy, B., et al.: 1999, "Images of Neptune's ring arcs obtained by a ground-based telescope", *Nature*, **400**, 731-733.
- Simó, C.: 2006, "Boundaries of Stability", Talk given at the Univ. de Barcelona. See <http://www.maia.ub.es/dsg/2006/index.html>.
- Simó, C.: 2007, "Studies in Dynamics: From local to Global aspects", Lecture given at the opening of the 2007-2008 course in the Societat Catalana de Matemàtiques (Barcelona). See <http://www.maia.ub.es/dsg/2007/index.shtml>.
- Simó, C., and Vieira, A.: 2007, "Global study of area preserving maps", in preparation.